Proceedings of the
International Conference on Mechanical Engineering 2011
(ICME2011) 18-20 December 2011, Dhaka, Bangladesh

ICME11-FL-036

COMPUTATION OF NON-LINEAR DYNAMIC DERIVATIVES AROUND A SPECIALISED DELTA WING CONFIGERATION

Christopher Pevitt and Firoz Alam

School of Aerospace, Mechanical and Manufacturing Engineering, RMIT University, Melbourne, Australia

ABSTRACT

The goal of this paper was to determine the feasible to accurately model stability and control derivatives using Computational Fluid Dynamics (CFD) applications. If successful, this would be the first step towards CFD being utilised as a more reliable tool in the development of aircraft. The test bed used for this paper was based on a specialised delta wing configuration. The analysis was completed using specialised meshing software, the flow simulation software (TAU) developed by the German Aerospace Agency (DLR) and the graphical interface Tecplot. The focus of the work was on the computation of the pitch oscillation in the interesting angle of attack range. The results found were promising, though they still indicated that further research in this field is required to ensure true dependability on CFD results. The recommendations found would help to ensure the progress of future findings.

Keywords: Computational Fluid Dynamics, CFD, Delta Wing, Tecplot, TAU, Stability and Control, Dynamic Derivative

1. INTRODUCTION

Computational Fluid Dynamics (CFD) simulations have been used to a significant extent in the development of aircraft.. As software capabilities and computing power have increased over time, the importance of and reliance upon, CFD simulations has similarly increased. The simulation results have progressively become more accurate and reliable. However the data provided by CFD simulations has had limitations. As such, the results of CFD simulations have never been relied on as the sole source of data. The results were always validated with additional testing, either via wind tunnel testing or flight tests, both of which are costly and time consuming. Also, these options were not always practical or suitable alternatives. Additionally, under certain flight characteristics the wind tunnel results did not entirely represent the true flow over the aircraft.

It is preferable if all flight characteristics are known before the full scale aircraft enters flight testing. Once full scale flight testing commences, it is very costly to make changes to the aircraft. Furthermore, unexpected aircraft handling during testing can be very dangerous. Therefore, it would be greatly beneficial to improve the reliability and accuracy of CFD testing which would reduce the necessity for additional alternative testing. This would help to reduces costs in addition to opening up possibilities for more detailed testing under the entire flight envelope of the aircraft.

With recent advances in the Aerospace industry, the demand and commonality of Unmanned Aerial Vehicles (UAV) has increased. These planforms often lead to configuration with nonlinear aerodynamic behaviour; this can be dominated by vortical flow across the upper surfaces. Many of the characteristics of flow phenomena associated with highly swept delta wings have been well documented [1]. However, the flow is not entirely understood in less swept wings with rounded leading edges. It is these characteristics that need to be better understood in order to effectively enhance future developments of aircraft and the use of CFD.

The determination of dynamic derivatives in aircraft development is an essential part of the development cycle in flight physics. When reviewing an unstable aircraft, knowledge of the stability and control margins are critical for design of the flight control systems. This is vital, as many future unmanned aircraft configurations exhibit aerodynamic stability and control issues in various regions of their flight envelope.

The goal of this paper is to focus on the computation of the pitch oscillations in the interesting AoA range. In conjunction with this an appropriately accurate static model will try and be achieved. During this process individual parameters will be assessed. These parameters will be altered with the goal of improving the static results and determining how they will relate to the dynamic model.

2. AERODYNAMICS OF DELTA WINGS

The Delta wing is a common design utilised in the development of supersonic aircrafts around the world [2]. There are a large number of delta wing types including; Standard, Ogival, Compound, Cropped, Tailless, Cranked Arrow and Diamond/Lambda configurations [3]. These configurations can be seen in Figure 1.

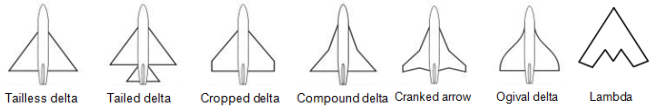

Fig 1. Delta Wing Configurations [3]

The delta wing configuration that is used for this paper is a Lambda type of delta wing with a 53º swept wing. In addition to the delta configuration, that sweep angle of the wings also characterizes the type of delta wing, between slender and non-slender. A non-slender delta wing is defined as having a sweep angle equal or less than 55º [1]. These are known as low sweep angle wings. This means the configuration used is also characterised as a low sweep angle, non-slender, lambda delta wing.

A method of characterising a slender delta wing is through its sweep angle. This consists of wings with a sweep angle equal or greater than 65º. The majority of testing that has been performed to date has been focused on slender delta wings. Due to this many aerodynamic investigations, examining the flow physics around this this type of configuration, have been conducted. As a result the flow phenomenon that is seen is quite well understood [4]. This type of configuration is often this is seen in modern day Jet fighters.

A non-slender delta wing is denoted as a delta wing with a sweep angle equal or less than 55º. Initial findings in computations and experimental studies revealed that at low AoA non-slender delta wings will form a "dual" primary vortex structure over the configuration [1]. Based on the work done by Gursul, it is noted that "this particular vortex structure is a result of the proximity of the vortex formation to the wing surface, and the corresponding interaction with the surface boundary layer". Other findings have come to the conclusion that this formation is unique to non-slender delta wings.

Another key feature of the non-slender delta wing is that the flow separation and the formation of the vortices will occur at very low AoA. The complete vortex development will not develop until higher AoA. As the vortical flow forms over the wing surface, the vortices will interact with the boundary layer. This will result in the formation of a dual vortex system [1].

3. MODEL CONFIGURATION

The model is a specifically designed UCAV delta wing configuration. It was developed for research purposes as part of the NATO, RTO task group. The model has been specifically designed in order to develop key aerodynamic characteristics such as flow separation and the development of vortices. The exact configuration used can't be shown due to current confidentially restrictions. The model has a 52º swept leading edge with the capability of interchanging a sharp or rounded leading edge. For this paper, the rounded leading edge will be used. The rounded leading edge configuration is created with a sharp inboard leading edge which transitions into a medium round leading edge on the outer panels of the wing. The outer panel has a parallel leading and trailing edge with a washout twist of 5º [6].

The model consists of three main sections; the fuselage, the wing section and wing tips. It is made of a light weight reinforced plastic that brings its overall weight to less than 10 kg [7]. The purpose of the extra light model is that it reduces the dynamic inertial loads. This allows for a more accurate and sensitive balance, which leads to better force and moment resolution. The model consists of more than 200 pressure taps on the upper and lower side of the model which are set to determine the dynamic measurements of unsteady pressure. The model was designed to gather both static and dynamic results.

4. COMPUTATIONAL PROCEDURE

The Flow simulation software that was used in this paper was the DLR TAU-Code. This is a software package developed by the DLR Institute of Aerodynamics and Flow technology. It was designed to be capable of solving complex CFD simulations. The solver is based around the compressible three-dimensional, steady, and unsteady Reynolds Averaged Navier-Stokes equations [8]. For this paper, an unstructured grid will be used that is developed with an in-house meshing program called "Mesher". The TAU-Code has the capabilities to utilise both the Cell-Vertex and the Cell-Centered schemes, both with their own advantages and disadvantages. For this paper, the Cell-Centered scheme was used. In the Cell-Centered approach, the Navier-Stokes equations are solved on a dual background grid, which is determined directly from the primary grid [9]. This approach was used as it consists of a larger number of solution variables than other approaches, which would in turn lead to greater accuracy. The TAU-Code is capable of performing many different tasks and these can be split into five main modules. These modules can be seen as [8]:

a) Preprocessor – Takes information from the Primary grid to develop a dual-grid or multi-grids.

b) Solver – Performs the flow calculations over the dual-grid.

c) Adaption – Refines and de-refines the grid to allow for the capture of all flow phenomena. This includes a large range of categories, including the representation of vortex structures and shear layers around viscous boundaries.

d) Deformation – Propagates the deformation of surface-coordinates to the surround grid.

e) Motion – Defines the motion of the model and relates this motion to any control devices.

Many of these modules are inbuilt within the code and for this paper; they will not be altered from their default values. As a result, the Preprocessor and Solver modules will be examined in more detail while the other modules will be taken as non-variable. The Pre-processor

module is based on the meshed grid forming the primary grid. For this paper, a system of five dual grids was used. This introduction of multiple grids greatly improves the computational time and power required to run any simulation. The Solver module calculates the gradients in time, which are then discretised through the use of a multi-step Runge-Kutta scheme. These calculations are then calculated using multigrid techniques and local time stepping which accelerates the ability to find converged results for steady state solutions [9].

5. NUMERICAL RESULTS

5.1 Pitching Oscillations

An essential part of this paper was to determine the feasibility of modelling dynamic derivatives in CFD. The dynamic derivatives help to characterise the aircraft in respect to its stability and control properties. It is an essential part of the development cycle in flight physics. With modern aircraft it is often necessary to design unstable aircraft configurations, making the knowledge of the stability and control margins central for the design of the flight control systems. For many different reasons it can be desirable to develop unstable aircraft such as reducing radar cross section. This concept of unstable design also applies to the configuration used in this work. In the scope of this paper the goal was to be able to model the dynamic pitching coefficient of the aircraft under amplitude changes of ±5º with a pitching frequency of both 1Hz and 3Hz.

The initial tests that were performed were based on the statically determined model. A range of tests were performed by changing different parameters of a static model to firstly try and gain the optimal static design. Initial dynamic test were performed based on the initial static results. These static results were based on a model with a mesh refinement of 10.5 million nodes and run using a SAE turbulence model. These initial static results and experimental results can be seen along with the dynamic data in Figures 5 to 10. The reason this model was used first, rather than a more refined model, is that the dynamic tests run in parallel to the static ones. This means that when the testing began, the findings of a more refined model had not yet been made. The effect of the more refined model will be looked at later in the report.

The first step in the calculation of the dynamic pitch oscillations is to find the moment and force graphs associated with each run. This is done based on the static solution found from the 10.5 million node models. The solution outputs for 5º, 10º, 15º and 25º were taken. Then each of these models was re-run under dynamic pitching oscillations. Each model was run with amplitude of ±5º with the first testing being done at 1Hz. This was chosen for initial testing as in previous studies it was noted that the slower frequencies was harder to model accurately. The reason that slower frequencies are harder to model is that the lower frequencies undergo more non-linear behaviour. It is expected that this is due to the flow dynamics having enough time to transition between states at lower frequencies. For higher frequencies the flow will not have enough time to transition, this causes a more linear behaviour [10].

The dynamic simulations were run using the same parameter settings as the static runs they started from. Each cycle that was run consisted of 100 iterations with 100 inner iterations. Each model was run for a total of 3 cycles to ensure the results were well converged. In order to run the simulations at 1Hz the TAU inputs corresponded to a reduced frequency for rotation of 0.06. These simulations were run and provided dynamic force and moment graphs**.** These results can be seen in Figure 8 to Figure 10. The equivalent experimental data that corresponds with these values can be seen in Figures 5 to 7.

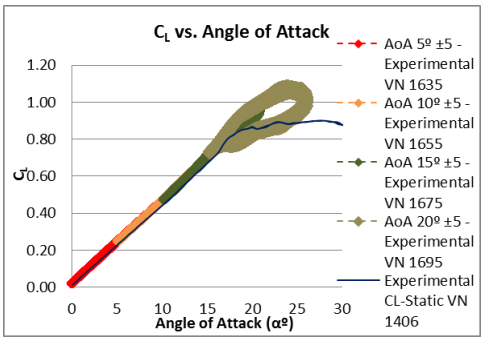

Fig 5. Experimental Data - C_L vs. Angle of Attack

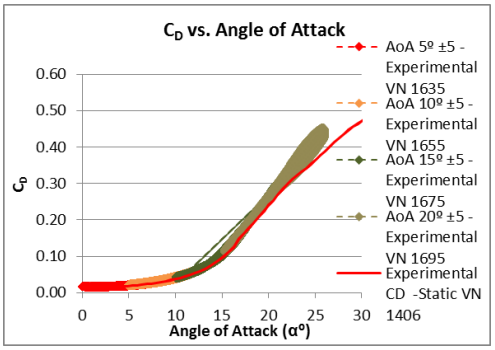

Fig 6. Experimental Data - C_D vs. Angle of Attack

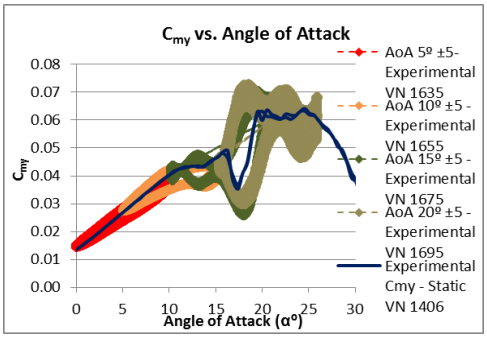

Fig 7.Experimental Data - C_{my} vs. Angle of Attack

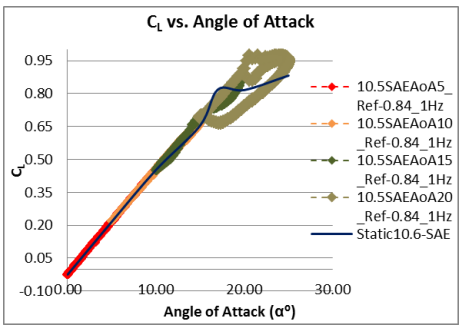

Fig 8. Dynamic Tests, for 5º, 10º, 15º and 20ºwith ±5º - C_L vs. Angle of Attack

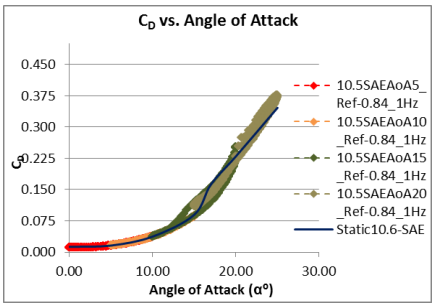

Fig 9. Dynamic Tests, for 5º, 10º, 15º and 20º with ±5º - C_D vs. Angle of Attack

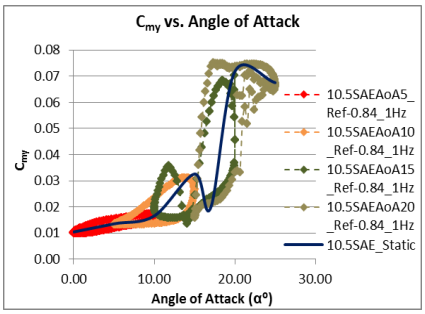

Fig 10. Dynamic Tests, for 5º, 10º, 15º and 20º with ±5º - C_{my} vs. Angle of Attack

From the dynamic results seen in Figure 8 to Figure 10 it can be seen that the most complex and least linear results are seen in the pitching moment characteristics. It is also seen when comparing the results to the experimental values that there is the least amount of agreements in the results for the pitching moment coefficients. As a result of this the pitching moment results will be review for further testing and analysis. It can be noted that the improvements in pitching moment results will coincide with improvements in the coefficients of lift and drag results.

The dynamic simulation results (not shown here due to space limitations) for the pitching moment shows that there are large deviations in the results. This was expected, as the static results had such large deviations compared the experimental results. It has been seen that the dynamic results will follow the static results all the time so high level of accuracy were not expected for the dynamic C_{my} values. Though when reviewing the C_L and C_D dynamic graph it was seen that for all AoA, even where the results deviated from the experimental ones, the flow phenomena was still captured. The simulation data still showed the same shape and characteristics as the experimental data. When reviewing the dynamic C_{my} values it was seen that the vales were not only translated away from the experimental results but the flow shape and characteristics were not the same.

The prelimenary dynamic simulation results indicated that the model will follow the static model results (not shown here) and further mesh refinment is required to ensure improved accuracy.

Therefor two additional models were tested. One was based on the 22.5 million nodes, half model with sting, and the other was based on the same model with both dissipation and preconditioning parameters altered o better capture the flow. The goal from this was to try and match testing with the static results that were being solved in unison. Though despite several attempts, a simulation could not be made that would allow for the solution to finish when both the preconditioning and dissipation parameters were in place. These models would results in failure due to numerical errors. Simulations were then performed on both preconditioning and dissipation separately. It was then found that it was the dissipation input leading to numerical errors, meaning changes in the dissipation parameters could not be made.

When the preconditioning was used, it was found that model would work, but under the current parameters would not converge with in its inner time steps. To try and help the process the model was rerun with precondition and the inner time steps were increased to 400. This improved the convergence greatly but still did not fully converge the results. Due to this, the preconditioning was not used for further studies. To indicate the quality of both the standard 22.5 million node model and the addition of precondition the Cmy graphs for both at 20º can be seen in Figure 11.

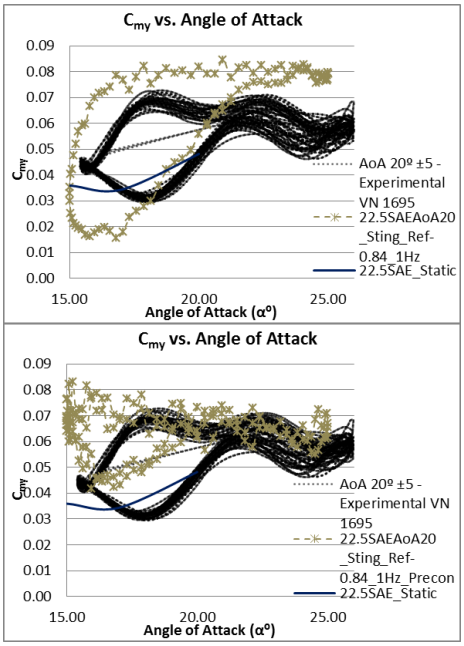

Fig 11. Experimental Data vs. Dynamic Tests, at 20º for Standard 22.5 million nodes (top) preconditioning (btm)

From the results in Figure 12 it was seen that the additional mesh refinement changed the shape of the C_{my}

dynamic graph but did not improve its overall accuracy. Due to this, a detailed decision of its benefits could not be made without further testing of additional AoA. When looking at the preconditioning model it appears that the results not only improved greatly but would follow the characteristics of the flow very well. As these results would not fully converge it was not possible to use them. It is expected that with additional time steps this model would converge further and would result in the more accurate results. Although with the available computational power and time frame available it was not possible to further refine the time steps on this model to determine the possible accuracy. It would be recommended for future tests that this be explored as it may lead to a greater quality result. As a result of the convergence problems, further testing was done on the 22.5 million nodes, half model with sting. Additional tests were performed at 10 and 15º. The results from all of these tests can be seen in Figure 12.

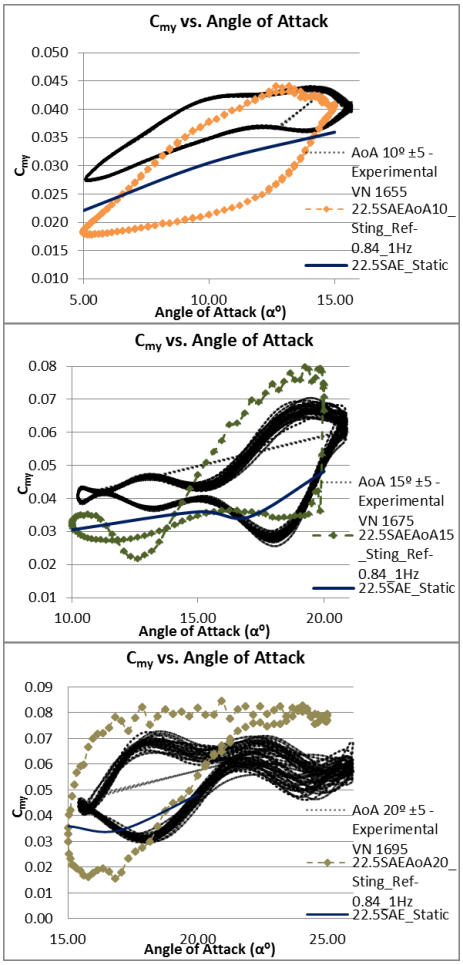

Fig 12. Experimental Data vs. Dynamic Tests - C_{my}, for 10º,15º and 20º with ±5º

The effect of the 22.5 million nodes mesh is more noticeable for the pitching moment graphs in Figure 12. When looking at the solution at 10º it can be seen that due to the improvements in the static results the dynamic results have translated up noticeably and are now much closer to the experimental data. The characteristics of the flow have also improved, though as this is an area of the complicated flow, the characteristics indicated are still very different to the experimental data. It is expected that being able to get the preconditioning and dissipation parameters to work would allow for this characterisation of the flow to be modeled in greater detail.

For the Dynamic C_{my} values at 15º degrees it can be seen that the improvement in the static results have once again caused the dynamic results to translate upwards again. This improves the results of the dynamic graph. Additionally the graph is now represented by the flow characteristics better than it had before. Though it can still be seen that on the downwards stroke (or the top line) the results dip and fall below then upwards stroke line. This characteristic is not present in the experimental data. As mentioned early the 22.5 million node model begins to merge its leading edge and thickness vortice earlier then what is desired. This effect would be the results of the dip in the results. It was seen that for the static results, this was improved when preconditioning and dissipation parameters were added to the solution. Therefore, it is expected that if the dynamic simulation could be run with these parameters, this dip in the results would be attended to, making the characteristic of the flow more accurate.

The 20º Dynamic C_{my} results indicate that the solution was again translated up as a result of the new static solution. Overall, the accuracy and characteristics of the flow in this region does not change a lot. The results on the lower AoA side around 15º have become closer to the experimental results due to the upwards translation of the graph. At the same time, the upwards translation has caused the results around 25º to move away from the experimental results slightly. In both the 10.5 million node model and the 22.5 million node model the characteristics of the flow do not change dramatically. Based on the one 1Hz results it was found that the 22.5 million node model did provide the most accurate results but was still lacking as it still did not fully characterise the dynamic flow across all of the AoA. It is believed that with the addition of the dissipation and preconditioning parameters the quality of the results would noticeably improve.

In addition to these test, some initial testing was performed on models pitching a 3Hz oscillation. These models were also run in unison to both set of testing. Due to this and because of a lack of time available the 3Hz model testing was performed on the 9.6 million node model with a k-ω turbulence model.

It was found that this was a much less accurate model then the 22.5 million node SAE model when looking at the static results. After this conclusion was realised it was too late to re solve the work with the better mesh. Despite this the force and moment results for the 3Hz testing can be seen in for 10º and 20º. By placing the model in a 3Hz oscillations the reduced frequency for rotation was reduce to 0.196. The pitching moment results can be seen in Figure 13.

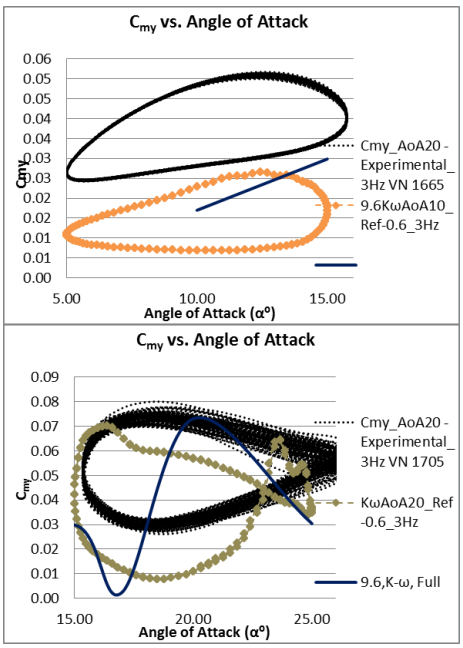

Fig 13. Experimental Data vs. Dynamic Tests at 3Hz, for 10º and 20º with ±5º

Despite the 3Hz model being based on a much less accurate model, Figure 13 illustrates that the majority of the results were quite similar to the experimental data**.**

When reviewing the C_{my} dynamic data, it was seen that at 10º the 3Hz still struggles to model the results accurately. It appears that the 10º C_{my} graph is the hardest to model for both 1Hz and 3Hz. For the 3Hz graph the flow characteristics and values are much closer then what was seen in the 1Hz graph. Overall the graphs are still quite different compared to the experimental data for 3Hz. It is expected that if the more refined model with precondition and dissipation was used for the 3Hz graph the results would be even closer. Unfortunately it can't be known exactly how accurate they could get at this time.

For the 20º results the simulation data is quite close to the experimental data. The graph appears to represent the flow characteristics accurately but is translated down. It is known that this downwards translation is due to the less accurate static data. So it is believed that the results would improve greatly with the used of the 22.5 million node mode with preconditioning and dissipation.

Over all it was seen that the 3Hz data was much easier to model then the 1Hz data. Even using a much less accurate static model the results were both quite accurate and indicated a good characterisation of the flow. Based on the results seen it is believed that with the use of the 22.5 million node model with preconditioning and dissipation the results would be very accurate.

It is assumed that with an appropriate static model it would indeed be possible to accurately model the dynamic derivatives of the configuration for higher frequency pitching oscillations.

6. CONCLUSION

Studies were completed at 1Hz and were based on the original 10.5 million node model. Initial findings indicated that the dynamic results in all force and moment graphs were directly related to the static results of the same model. Therefor high levels of accuracy were not possible unless the static models were also improved. Despite their variances in numerical values the C_L and C_D results were capable of accurately indicating the flow characteristics, while the C_{my} results appeared to vary both in numerical results and flow characteristics, epically in the region of flow separation.

Both the numerical results and the flow characteristics were improved for the mesh refined models. These improvements indicated dramatic beneficial changes in the flow characteristics at all AoA.

Based on the current accuracy of the dynamic models, the additional model refinement is clearly needed. As the dynamic results follow the static finding exactly, improvements made in the static results would greatly improve the dynamic results. It would be suggested that at the current accuracy levels, it would not be possible to model the 1Hz data in good confidence. At the same time it was seen that the 3Hz results could be modelled in quite good confidence as only slight deviances were seen in the C_{my} resulting at 10º to 17º AoA.

7. ACKOWLEDGEMENT

The author is highly grateful to Dr. Stephan Hitzel and Dr Herbert Rieger, from CASSIDIAN – Air systems for his assistance and support with the organisation and preparation of this work. As well as for their time and effort spent in ensuring it was produced to a high standard

7. REFERENCES

[1] Gursul, I., Gordinier, R., and Visbal, M. "*Unsteady Aerodynamics of Nonslender Delta Wings".,* s.l. : Elsevier Ltd., 2005.

[2] Century of Flight, "Development of Aviation Technology - Delta Wings", 2010, [cited January.2011] Available from: http://www.century-of-flight.net/

[3] Surruno, "Pakistan Defence - Wing Planforms" , 2009, [cited January.2011] Available from: http://www.defence.pk

[4] Visbal, M.R., "Computational and Physical Aspects of Vortex Breakdown on Delta Wings", Reno, NV:s.n., 9th -12th January 1995. 33rd AIAA Aerospace Sciences Meeting and Exihibit

[5] Gursul I., "Recent Developments in Delta Wing Aerodynmaics", The Aeronatical Journal, September 2004.

[6] Frink, N.T., "Strategy for Dynamic CFD Simulations on SACCON Configuration," AIAA Paper 2010-4559, June.2010.

[7] Vicroy, D.D., Loeser, T.D., Schütte, A., "SACCON Forced Oscillation Tests at DNW-NWB and NASA Langley 14X22-foot Tunnel", AIAA Paper 2010-4394, June.2010

[8] Schütte, A., Hummel, D., Hitzel, S.M., "Numerical and experimental analyses of the vortical flow

around the SACCON configuration" AIAA Paper 2010-4690, July, 2010.

[9] Hübner, A.R., "Experimental and Numerical Investigations of Unsteady Aerodynamic Derivatives for Transport Aircraft Configurations" AIAA Paper 2007-1076, January, 2007.

[10] Rohlf, D., Schmidt, S., Irving J., "SACCON Stability and Control Analysis Applying System Identification Techniques", AIAA Paper 2010-4399, June.2010

8. NOMENCLATURE

Symbol	Meaning	Unit
C_D	Coefficient of Drag	-
C_L	Coefficient of Lift	-
C_{my}	Coefficient of Pitching Moment	-
C_p	Coefficient of Pressure	-

9. MAILING ADDRESS

Mr Christopher Pevitt
School of Aerospace, Mechanical and Manufacturing Engineering
RMIT University, Plenty Road, Bundoora
Melbourne, VIC 3083, AUSTRALIA
Phone : (+61) 0423 031 275
FAX : (+613) 9925 6506.
E-mail : christopher.pevitt@student.rmit.edu.au